

# First-principles calculation and scanning tunneling microscopy study of highly oriented pyrolytic graphite (0001)

E. Cisternas,<sup>1</sup> F. Stavale,<sup>2,3</sup> M. Flores,<sup>4</sup> C. A. Achete,<sup>2,3</sup> and P. Vargas<sup>1,5,\*</sup>

<sup>1</sup>*Departamento de Física, Universidad Técnica Federico Santa María, P.O. Box 110-V, 2340000 Valparaíso, Chile*

<sup>2</sup>*Divisão de Metrologia de Materiais (DIMAT), INMETRO, CEP 25250-020 Duque de Caxias, RJ, Brazil*

<sup>3</sup>*Programa de Engenharia Metalúrgica e de Materiais (PEMM), Universidade Federal do Rio de Janeiro, Cx. Postal 68505, CEP 21945-970 Rio de Janeiro, RJ, Brazil*

<sup>4</sup>*Atomic Physics Laboratory, RIKEN, Wako, Saitama 351-0198, Japan*

<sup>5</sup>*Max-Planck Institute for Solid State Research, Heisenbergstrasse 1, D-70569 Stuttgart, Germany*

(Received 10 March 2009; revised manuscript received 7 May 2009; published 29 May 2009)

In this work we report a theoretical and experimental study of the HOPG(0001) surface using density functional theory and scanning tunneling microscopy (STM) where both the triangular and the full hexagonal atomic structures are resolved. The experimental STM images are supported by *ab initio* charge-density calculations and STM image simulations without invoked mechanical or electronic tip effects. The optimal experimental conditions to obtain both structures are discussed in detail.

DOI: [10.1103/PhysRevB.79.205431](https://doi.org/10.1103/PhysRevB.79.205431)

PACS number(s): 71.15.Ap, 68.37.Ef, 81.05.Uw

## I. INTRODUCTION

Despite that for several years the highly oriented pyrolytic graphite HOPG(0001) surface has been theoretically (by calculating the electronic structure) and experimentally [by using scanning tunneling microscopy (STM)] studied,<sup>1–22</sup> some important issues are not yet well understood. The fact that in most STM images are observed only three of the six carbon atoms from the hexagon of the graphite top-layer lattice,<sup>1,2</sup> “giant corrugations” (enormous apparent heights of atoms)<sup>3</sup> and giant hexagonal periodic patterns (referred as moiré patterns)<sup>4–8</sup> have attracted a lot of scientific interest and have been the starting points to propose several hypotheses to explain these phenomena. These hypotheses have a wide range of physical grounds and among those it is possible to find the mechanical tip-to-sample interaction,<sup>9</sup> multiple mini tips,<sup>10</sup> subsurface defects,<sup>11</sup> and the surface charge-density picture.<sup>12</sup> However, none of these hypotheses gives a completely satisfactory explanation to understand the STM image formation mechanism on this surface. This fact is particularly important, since the scanning tunneling microscopy is one of the crucial experimental techniques to investigate surface defects, such as terraces,<sup>13</sup> and the novel properties of quantum structures based on graphene (see next paragraph) as quantum dots and nanoribbons.<sup>14</sup>

Basically, the highly oriented pyrolytic graphite (HOPG) crystal is formed by layers of honeycomb atomic array of carbon atoms with interatomic distance of 1.42 Å (a single layer is called graphene). The layers are held together by van der Waals forces and they present an ABAB stacking sequence. This stacking sequence gives rise to a 4-carbon atom unit cell with two nonequivalent atomic sites: the  $\alpha$ -type-sites, atoms with neighbors directly above and below in adjacent layers, and the  $\beta$ -type-sites, atoms without such neighbors<sup>15</sup> (in what follows  $\alpha$  and  $\beta$  atoms, respectively).

The widely accepted theory for STM image formation of Tománek *et al.*<sup>12</sup> predicts, for low-bias voltages, that only  $\beta$  atoms are visible as a consequence of the asymmetry in the interlayer interaction in the bulk graphite. Such asymmetry

occurs due to the higher local density of states (LDOS) of the  $\beta$  atoms compared with  $\alpha$  atoms near the Fermi level. This (often called triangular) electronic surface structure has a unit cell length of about 2.46 Å corresponding to the periodicity of the lattice, and it is usually reported in the STM experiments.<sup>1,2</sup> In this way, the authors in Ref. 12 explain the usually found experimental STM image features at low-bias voltages. However, despite this successful explanation, tip-size effects must be invoked to understand the persistence of the triangular structure at higher voltages since the calculations predict that the LDOS, and consequently the tunneling current, for  $\alpha$  and  $\beta$  atoms tend to be equal by increasing the bias voltage.

To elucidate this fact, the three other *invisible* carbon atoms have been sought for several researchers during the last seventeen years,<sup>16–22</sup> but since it is not possible to control the sharpness of the tip no definite conclusions have been achieved. Even so, Hembacher *et al.*<sup>16</sup> obtained very interesting results using a low-temperature highly sensitive STM/atomic force microscopy (AFM) setup and revealing the full hexagonal structure by AFM. Another initiative using scanning tunneling microscopy at room temperature by Wang *et al.*<sup>17</sup> reports STM images of both structures, the triangular and the hexagonal, which were obtained using the same tip. In this last report the occurrence of the full hexagonal structure was rarely observed (10%–20% of times) and these authors attributed the hexagonal structure to a mechanical layer-sliding model, early proposed by Ouseph *et al.*<sup>18</sup>

The main goal of the present study is to clarify the conditions required to observe the full atomic structure on HOPG(0001) surface, without mechanical or electronic additional considerations. Within this framework we imaged HOPG at room temperature using STM where both structures (triangular and hexagonal) at different feedback conditions are obtained. The STM image features are interpreted from spatial charge density based on first-principles linear muffin tin orbital (LMTO) calculations. The experimental data are in agreement with these calculations and the results indicate a strong image-feature dependence on the tip-to-surface distance.

## II. THEORETICAL APPROACH

In order to obtain the simulated STM images we have computed the charge density above the HOPG(0001) surface using first-principles total-energy electronic structure calculations within the density functional theory (DFT) (Refs. 23 and 24) and the local density approximation (LDA). The LMTO method<sup>25,26</sup> under the atomic sphere approximation (ASA) was used for this purpose and the surface was simulated by a repeating four-graphene layer slab model (ABAB stacking sequence), where the slabs are substantially separated (16.8 Å) to avoid artificial interactions and to ensure that the charge density goes to zero effectively far from the surface. The density of states (DOS) in this configuration has been calculated for atoms on the top surface and internal layers. In addition and for comparison, the DOS for HOPG bulk (filling all the space with carbon atoms) was calculated with the same method and accuracy. The DOS from atoms of internal layers in the slab and bulk configuration show similar structure and both cases are in agreement with previous results,<sup>27</sup> showing additionally that the DOS near the Fermi energy for  $\beta$  atoms is larger than those for  $\alpha$  atoms.

The spatial charge density computed with this method was used in the expression for tunneling current-density  $j(\mathbf{r})$  showed in Eq. (1), which is a simple extension<sup>28</sup> of the expression of Tersoff and Hamann,<sup>29</sup>

$$j(\mathbf{r}, V) \propto \int_{E_F - eV}^{E_F} \rho(\mathbf{r}, E) dE \quad (1)$$

where

$$\rho(\mathbf{r}, E) = \sum_{n,k} |\Psi_{n,k}(\mathbf{r})|^2 \delta(E - E_{n,k}) \quad (2)$$

Here,  $\rho(\mathbf{r}, E)$  is the LDOS at the tip center position  $\mathbf{r} = (x, y, z)$ , the  $\Psi_{n,k}(\mathbf{r})$  are the eigenstates of the unperturbed surface with corresponding energy  $E_{n,k}$ , and  $V_b$  is the applied bias voltage to the tip sample. Thus, to perform our calculations of the electronic charge density participating in the tunneling we integrate the electrons that are within the energy window  $[E_F - e|V_b|, E_F]$ . By defining the axis perpendicular to the graphite surface as the  $z$  axis and setting a constant value for  $z$ , it is possible to generate the spatial charge density over  $xy$  plane, which is proportional to STM current image. The tip-size effect has been considered by performing a lateral and uniform smoothing with radius of about 1.0 Å (Ref. 30) of the charge density.

## III. EXPERIMENTAL SETUP

The experiments were performed using a variable temperature scanning tunneling microscopy (VT-STM) from Omicron with background pressure better than  $10^{-10}$  mbar. The samples were peeled off using an adhesive tape in air and transferred into the vacuum chamber. The STM images were collected at room temperature at both modes (constant current and constant height) using etched tungsten tips. The bias voltages refer to the applied sample bias, which corresponds to the filled states. The scans direction was performed from the bottom-to-up at all images. The images were flat-

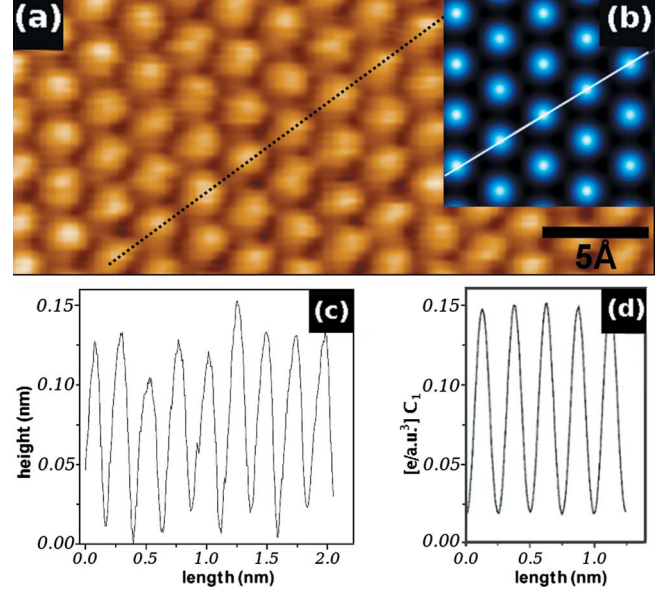


FIG. 1. (a) (Color online) Experimental STM image of HOPG at constant-current mode,  $V_b = -50$  mV. (b) Calculated STM image at constant-height mode,  $V_b = -50$  mV, and tip-surface distance of 1.2 Å. The triangular structure is visualized in both images. (c) And (d) line profiles along the lines indicated in Figs. 1(a) and 1(b), respectively.

tened to correct the sample tilting and filtered with smooth filters.

## IV. RESULTS AND DISCUSSION

The usually reported experimental HOPG STM image with atomic resolution is presented in Fig. 1(a). Here the triangular structure is visualized from one of the lattice sites. This image was obtained in constant-current mode, with  $I_t = 0.4$  nA and  $V_b = -50$  mV. Figure 1(b) shows a calculated STM image (constant-height mode) at the same bias voltage, with  $z = 1.2$  Å. The line profile (LP) along the lines indicated in Figs. 1(a) and 1(b) are presented in Figs. 1(c) and 1(d), respectively, where the vertical axis in the last one has been adjusted by introducing a multiplicative constant  $C_1 = 4.0 \times 10^{-4}$ . Both profiles might be compared assuming that depressions in the charge density lead to proportional approximations of the tip-to-the-surface in order to keep the tunnel current constant. Accepting this fact, the agreement is quite well between theory and experiment, and with early reports also.<sup>1,2</sup> Besides, the atomic corrugation revealed from the experimental LP is around 1.2 Å value which corresponds to the atomic corrugation informed by Mamin *et al.*<sup>3</sup> for STM graphite characterization under UHV and clean conditions. This fact indicates that contaminants do not exist on the tip.

Figure 2(a) and inset (low left corner) show experimental current STM (at constant-height mode) images that exhibit the HOPG surface's full atomic structure. Here, the tunnel current range goes from  $\sim 0.1$  up to 2.0 nA and is taken at  $V_b = -300$  mV. The simulation was performed [shown in Fig. 2(b)] at the same bias voltage, considering a constant tip-to-surface separation of 1.2 Å. Experimental and simulated im-

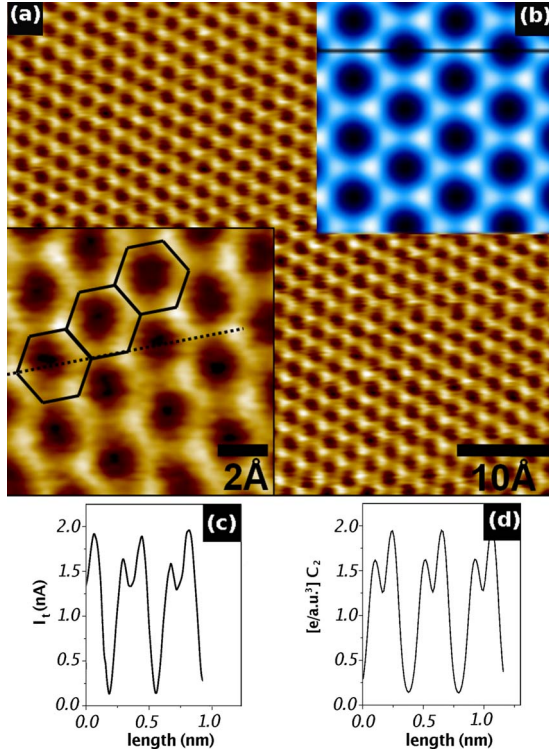


FIG. 2. (a) (Color online) Experimental STM image of HOPG at constant-height mode,  $V_b = -300$  mV. (b) Calculated STM image at constant-height mode,  $V_b = -300$  mV, and tip surface distance of 1.2 Å. Both images reveal the hexagonal atomic structure which is compound by  $\alpha$  and  $\beta$  atoms. (c) And (d) are line profiles along the lines indicated in (a) and (b), respectively.

ages show current maxima on three of the six carbon atoms of the surface-hexagonal ring (eye-guide hexagonal net was inserted on the experimental image). From the calculated image are easily identified the carbon atoms on each lattice site and thus it was stated that the brightest correspond to  $\beta$  atoms and the less intense are  $\alpha$  atoms. The same labels were extended at the experimental image. The central black regions in the hexagons correspond to the hollows sites.

We have performed LP along the line indicated over the experimental (simulated) image which is shown in Figs. 2(c) and 2(d). The multiplicative constant  $C_2 = 1.3 \times 10^{-4}$  was introduced [Eq. (1)] to scale the vertical axis for the Fig. 2(d) and to compare directly, and without additional assumptions, both results. Thus, the line profiles confirm that one kind of atom, the  $\beta$  atom, presents a higher current density, revealing a difference in the LDOS if we assume that all carbon atoms in the surface layer are in the same plane. Such difference was stated before for Tománek *et al.*,<sup>12</sup> who introduced the following asymmetry-definition  $A \equiv (j_\beta - j_\alpha) / (j_\beta + j_\alpha)$  to quantify the phenomenon. Replacing our experimental and theoretical data in this expression we find  $A = 0.13$  and  $A = 0.10$ , respectively. Both results present a pretty well agreement with the values calculated by Tománek *et al.*<sup>12</sup> for 0.3 V bias voltage and 0.5 and 1.0 Å as tip-to-surface separation.

The asymmetry between these two atomic sites was also shown previously by Atamny *et al.*,<sup>19</sup> but not clearly from

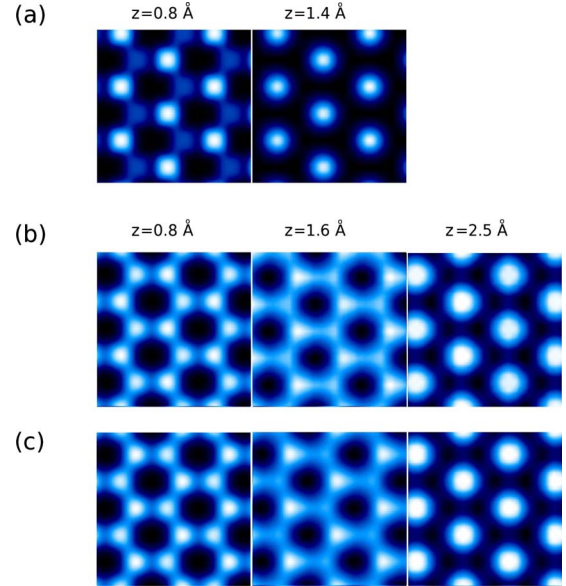


FIG. 3. (Color online) Calculated STM images representative of three different bias-voltage ranges: (a)  $-50$  to  $-200$  mV, (b)  $-300$  to  $-800$  mV, and (c)  $-1000$  to  $-1500$  mV: two different tip-surface separations for the first bias-voltage range and three tip-surface separations for the next two ones. The brightest spot indicates the maxima of charge density, and the asymmetry in intensity for different voltage and separation is illustrated.

the STM image. Actually they found such asymmetry from the line-profile analysis where they observed a shoulder around the brighter atom. This shoulder was attributed to the  $\alpha$  atom (Fig. 3 in Ref. 19). In our case, the set of parameters ( $V_b, I_t$ ) enables obtain high-resolution STM images and clearly resolve both atom sites and its corresponding asymmetry. Such STM image feature, site asymmetry, reveals clearly the graphite electronic structure instead of any possible graphene slide layer as it was proposed before.<sup>17,18</sup>

In order to clarify which conditions are needed to image the full hexagonal structure, we performed a set of theoretical calculations at  $V_b$  from  $-50$  mV up to  $-1.5$  V and  $z$  from 0.5 up to 3 Å at constant tip-surface distances. The representative results over those ranges are displayed in Fig. 3, where these theoretical images are separated in three different bias-voltage ranges (a)  $-50$  to  $-200$  mV, (b)  $-300$  to  $-800$  mV, and (c)  $-1000$  to  $-1500$  mV. At this point it is important to remark that current maxima declines exponentially if the simulated tip-to-surface separation is incremented (Fig. 3, from left to right). However, as it occurs in the experiments, contrast remains unaltered.

For the first calculated voltage range ( $-200$  mV  $< V_b < -50$  mV) series in Fig. 3(a), the brightness difference between  $\alpha$  and  $\beta$  atoms is strong, even when the tip is very close to the surface ( $z = 0.8$  Å). In addition, although the asymmetry diminishes for closer tip-surface separation, even so it is difficult to resolve both atoms. This explains, as it was stated by Tománek *et al.*,<sup>12</sup> why it is not possible to resolve both atoms at energies ( $eV_b$ ) close to Fermi energy during the STM image acquisition. On the other hand, the calculation predicts no image for  $z$  beyond 1.6 Å. This occurs because for smaller bias voltages the integral of spatial

charge density [Eq. (1)] diminishes and consequently falls below more drastically than for higher voltages.

For the two following bias-voltage range series of Figs. 3(b) and 3(c), the brightness difference (asymmetry) between  $\alpha$  and  $\beta$  sites diminishes, i.e., charge-density differences are getting smaller by increasing the applied bias voltage (energy window). As it is well-known, this behavior was predicted before,<sup>12</sup> being the usually triangular STM HOPG(0001) structure attributed to tip-size effects. Additionally, for these voltage ranges the calculated charge density spreads beyond 2 Å, and beyond this value these theoretical results predict that only one brilliant spot per unit cell would be visible.

Based on the theoretical experimental image features, the bias voltage and the tip-to-surface separation  $z$  are physically important in order to obtain the triangular or the hexagonal surface structures. The overall experimental data analysis indicates that the full hexagonal atomic structure was successfully resolved at  $V_b = -200 \sim -300$  mV and  $I_t = 1.5 \sim 3$  nA, and in general at constant height mode. Although our theoretical results do not match exactly with the experimental bias-voltage range to achieve full atomic resolution (probably due to thermal effects),<sup>31</sup> there exists an agreement related to a windows energy ( $eV_b$ ) very close to the Fermi energy, where full resolution is not possible. On the other hand it is expectable that for high experimental bias voltages the tip deals with high tunnel currents. This phenomenon during the image acquisition represents an inconvenience for bias voltages larger than 300 mV, and fine adjustments must be made in order to preserve such full atomic resolution. Anyway, the theoretical simulated images show that the asymmetry depends strongly on the tip-surface separation and that, for bias voltages not so close to the Fermi energy, the full resolution can be achieved [Fig. 3(b)] if the tip is sufficiently near to the sample.

Thus, these calculations show that during a hypothetical image acquisition with the tip approaching continuously to the surface (polarization-voltage constant, over 200 mV and biased positively with respect to the sample), it will detect first a tunneling-current maximum over only one lattice site, until the tip finally reaches the zone where the two atoms appear visible with their respective asymmetry. Therefore, if full resolution is obtained in a STM experiment, a triangular structure can be imaged after a tip retraction.

Under this scheme we performed STM experiments scanning the surface at constant-height mode, but with the particularity that the tip-to-surface separation was suddenly changed (maintaining the bias-voltage constant). In this way we obtained an image divided into two zones, each one recorded for a different tip-to-surface distance. Using such procedure to go from the hexagonal to the triangular structure we retract the tip about 1 Å (1 Å refers to a nominal distance value set at the piezo which corresponds to current decrease of approximately 0.7 nA) and these results are displayed in Fig. 4. There it is clearly visible how both structures are resolved and, according theoretical predictions, how for a larger tip-to-surface separation only one maximum appears. Similar features were observed in the inverse experiment (not shown here), during which the full structure was recovered by approaching the tip during the current-image acquisition.

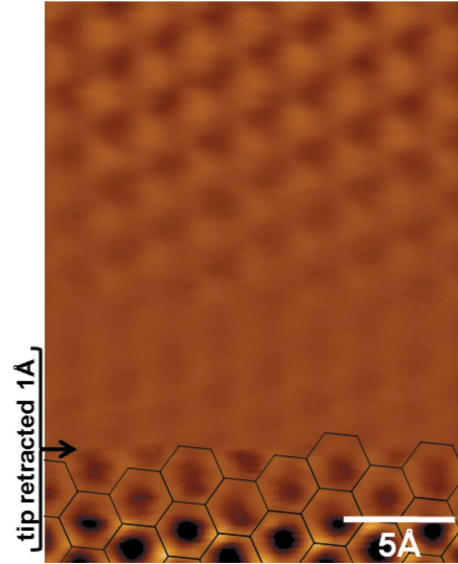


FIG. 4. (Color online) Experimental STM image of HOPG at constant-height mode,  $V_b = -200$  mV and initial  $I_t = 2.1$  nA; sudden change of tip-surface distance to 1 Å far away. The image shows the transition from the honeycomb to triangular atomic structure by adjusting the tunneling current. The honeycomb lattice is superposed on the image to identify the bright spot positions.

As reported before,<sup>12</sup> these results indicate that the spatial charge-density distribution has its origin on the structural-asymmetry and graphene-interlayer interaction rather than on tip-size effects or any sort of mechanical interactions. Besides, the fact that the same tip produces both kinds of structures reflects the strong influence from the bias voltages (occupied states contributing to the tunneling current) and also from the tip-surface separation (probably due to surface states).<sup>32</sup> Thus it seems necessary to perform more experiments, perhaps combining STM with AFM (Ref. 16) to elucidate which site appears visible in the STM (Refs. 17, 20, and 21) at different bias voltages and tip-surface separation.

## V. FINAL REMARKS

In general, measurements in constant-height mode are more difficult to be performed compared with those in constant-current mode due to the obvious nonfeedback scan. However, the constant-height mode is particularly important in order to achieve the full hexagonal graphite structure. This mode reveals the full hexagonal structure according to our theoretical predictions based on DFT.

The simulated images clarify the physical meaning of such needed experimental conditions to achieve the full atomic structure due to the narrow ranges of tip-surface distance and bias voltage. In principle atoms on  $\alpha$ - and  $\beta$ -lattice sites can be imaged simultaneously if the asymmetry is small enough, a situation which occurs for a narrow set of experimental conditions. In addition, an important consequence is that tip-size effects would not ever be relevant in explaining the triangular structure, although we recognize that this parameter is left as an uncontrolled variable on the experiments.

It is well-known that Mizes *et al.*<sup>10</sup> developed theoretic-experimental studies to explain several patterns on the HOPG surface, including the hexagonal lattice. In this task they introduced a nonideal tip, specifically a double-atom tip, where amplitude and phase are chosen to match the character of experimental images. However, it is necessary to remark that neither tip-to-surface distances nor different bias voltages were considered in these studies. If such approximation would apply to our experimental results, one must pay attention to the line-profile asymmetry revealed from our theoretical and experimental results and at least it should be recognized that such site-current asymmetry [Figs. 2(a) and 2(c)] requires a very coincident double-tip configuration which is improbable to occur in each experimental image with full atomic resolution.

## VI. CONCLUSIONS

Experimental STM images of HOPG can be completely understood by performing standard DFT calculation of the

electronic charge density and Tersoff-Hamann model. In the ideal situation of a perfect tip, the full resolution of the hexagonal structure is predicted for voltages over 200 meV and tip-surface separation shorter than 2.0 Å. For smaller voltages and/or larger tip-surface separation the triangular structure appears. These statements were experimentally confirmed by showing that the kind of structure revealed has a strong dependence on the applied bias voltage and the tip-surface distance in a quite well agreement with the theoretical predictions.

## ACKNOWLEDGMENTS

F. Stavale thanks CNPq-PROMETRO and CAPES grants to support this work. P. Vargas thanks Millennium Science Initiative under Project No. P06-022-F and Fondecyt under Grant No. 1070224.

\*patricio.vargas@usm.cl

- <sup>1</sup>S.-I. Park and C. F. Quate, *Appl. Phys. Lett.* **48**, 112 (1986).
- <sup>2</sup>G. Binnig, H. Fuchs, Ch. Gerber, H. Rohrer, E. Stoll, and E. Tosatti, *Europhys. Lett.* **1**, 31 (1986).
- <sup>3</sup>H. J. Mamin, E. Ganz, D. W. Abraham, R. E. Thomson, and J. Clarke, *Phys. Rev. B* **34**, 9015 (1986).
- <sup>4</sup>M. Kuwabara, D. R. Clarke, and D. A. Smith, *Appl. Phys. Lett.* **56**, 2396 (1990).
- <sup>5</sup>J. Xhie, K. Sattler, M. Ge, and N. Venkateswaran, *Phys. Rev. B* **47**, 15835 (1993).
- <sup>6</sup>Z. Y. Rong and P. Kuiper, *Phys. Rev. B* **48**, 17427 (1993).
- <sup>7</sup>W.-T. Pong, J. Bendall, and C. Durkam, *Surf. Sci.* **601**, 498 (2007).
- <sup>8</sup>E. Cisternas, M. Flores, and P. Vargas, *Phys. Rev. B* **78**, 125406 (2008).
- <sup>9</sup>J. M. Soler, A. M. Baro, N. Garcia, and H. Rohrer, *Phys. Rev. Lett.* **57**, 444 (1986).
- <sup>10</sup>H. A. Mizes, S. I. Park, and W. A. Harrison, *Phys. Rev. B* **36**, 4491 (1987).
- <sup>11</sup>K. Kobayashi, *Phys. Rev. B* **53**, 11091 (1996).
- <sup>12</sup>D. Tománek, S. G. Louie, H. J. Mamin, D. W. Abraham, R. E. Thomson, E. Ganz, and J. Clarke, *Phys. Rev. B* **35**, 7790 (1987); D. Tománek and S. G. Louie, *ibid.* **37**, 8327 (1988).
- <sup>13</sup>Y. Niimi, T. Matsui, H. Kambara, K. Tagami, M. Tsukada, and H. Fukuyama, *Phys. Rev. B* **73**, 085421 (2006); Y. Niimi, H. Kambara, and H. Fukuyama, *Phys. Rev. Lett.* **102**, 026803 (2009).
- <sup>14</sup>K. A. Ritter and J. W. Lyding, *Nature Mater.* **8**, 235 (2009).
- <sup>15</sup>R. C. Tatar and S. Rabi, *Phys. Rev. B* **25**, 4126 (1982).
- <sup>16</sup>S. Hembacher, F. J. Giessibl, J. Mannhart, and C. F. Quate, *Proc. Natl. Acad. Sci. U.S.A.* **100**, 12539 (2003); *Phys. Rev. Lett.* **94**, 056101 (2005).
- <sup>17</sup>Y. Wang, Y. Ye, and K. Wu, *Surf. Sci.* **600**, 729 (2006).
- <sup>18</sup>P. J. Ouseph, T. Poothackanal, and G. Mathew, *Phys. Lett. A* **205**, 65 (1995).
- <sup>19</sup>F. Atamny, O. Spillecke, and R. Schlogl, *Phys. Chem. Chem. Phys.* **1**, 4113 (1999).
- <sup>20</sup>P. Moriarty and G. Hughes, *Appl. Phys. Lett.* **60**, 2338 (1992).
- <sup>21</sup>J. I. Paredes, A. M. Alonso, and J. M. D. Tascon, *Carbon* **39**, 476 (2001).
- <sup>22</sup>C. D. Zeinalipour-Yazdi and D. P. Pullman, *Chem. Phys.* **348**, 233 (2008).
- <sup>23</sup>P. Hohenberg and W. Kohn, *Phys. Rev.* **136**, B864 (1964).
- <sup>24</sup>W. Kohn and L. J. Sham, *Phys. Rev.* **140**, A1133 (1965).
- <sup>25</sup>O. K. Andersen and O. Jepsen, *Phys. Rev. Lett.* **53**, 2571 (1984).
- <sup>26</sup>O. K. Andersen, O. Jepsen, and D. Gloetzel, in *Highlights of Condensed Matter Theory*, edited by F. Bassani, F. Fumi, and M. P. Tosi, (North-Holland, New York, 1985); O. K. Andersen, O. Jepsen, and M. Sob, in *Lecture Notes in Physics: Electronic Band Structure and Its Applications*, edited by M. Yussouff, (Springer-Verlag, Berlin, 1987); O. K. Andersen, Z. Pawlowska, and O. Jepsen, *Phys. Rev. B* **34**, 5253 (1986).
- <sup>27</sup>J.-C. Charlier, X. Gonze, and J.-P. Michenaud, *Phys. Rev. B* **43**, 4579 (1991).
- <sup>28</sup>A. Selloni, P. Carnevali, E. Tosatti, and C. D. Chen, *Phys. Rev. B* **31**, 2602 (1985).
- <sup>29</sup>J. Tersoff and D. R. Hamann, *Phys. Rev. Lett.* **50**, 1998 (1983); *Phys. Rev. B* **31**, 805 (1985).
- <sup>30</sup>This value corresponds to the estimated tungsten atom radio.
- <sup>31</sup>At room temperature occupied states until 100 meV are notably perturbed.
- <sup>32</sup>M. Posternak, A. Baldereschi, A. J. Freeman, and E. Wimmer, *Phys. Rev. Lett.* **52**, 863 (1984).